THE ASTROPHYSICAL JOURNAL, 395:L49–L54, 1992 August 10

IMPLICATIONS OF ULTRAVIOLET IMAGING TELESCOPE OBSERVATIONS FOR STAR FORMATION HISTORIES IN NGC 1275

ERIC P. SMITH,[1,2] ROBERT W. O'CONNELL,[3] RALPH C. BOHLIN,[4] KWANG-PING CHENG,[1,2,5]
ROBERT H. CORNETT,[6] JESSE K. HILL,[6] ROBERT S. HILL,[6] PAUL HINTZEN,[1,2,7]
WAYNE B. LANDSMAN,[6] SUSAN G. NEFF,[1] MORTON S. ROBERTS,[8]
ANDREW M. SMITH,[1] AND THEODORE P. STECHER[1]
Received 1992 March 31; accepted 1992 May 28

ABSTRACT

We discuss UV imagery of NGC 1275 obtained using the Goddard Ultraviolet Imaging Telescope (UIT). We are able to study the UV morphology down to $\mu_{249} \sim 25$ mag arcsec^{-2}. There are significant non-axisymmetric structures in the UV continuum associated with the low-velocity filament system. Continuum from the high-velocity system may also be present. The large-aperture UV colors indicate that although the mass function extends to $\sim 5\ M_\odot$, more massive objects are not present. This implies either a cessation of star formation during the last $\sim$50–100 Myr or a truncated initial mass function.

Subject headings: galaxies: active — galaxies: individual (NGC 1275) — stars: formation

1. BACKGROUND

In addition to its bright radio emission, NGC 1275 (3C 84, Perseus A) has two distinct dynamical components, one at $cz = 8200$ km s^{-1} (the high-velocity [HV] system) and another at 5300 km s^{-1} (the low-velocity [LV] system; Minkowski 1957). Its nuclear emission-line spectrum is LINER-like, with evidence for an active galactic nucleus (AGN) (Seyfert 1943; Heckman, Miley, & Green 1984). Its global absorption-line spectrum is similar to that of an A star (Minkowski 1957), yet optical, UV, and infrared studies suggest that O and early B stars are absent (Wirth, Kenyon, & Hunter 1983; Sarazin & O'Connell 1983; Fabian, Nulsen, & Canizares 1984; Gear et al. 1985; Romanishin 1987). Its extended, filamentary Hα morphology of high luminosity is apparently not driven by stellar photoionization (Lynds 1970; Heckman et al. 1989; Caulet et al. 1992). The galaxy is centered in a massive X-ray–bright cooling flow with a mass deposition rate estimated to be $\dot{M} \lesssim 300\ M_\odot$ yr^{-1} (Fabian et al. 1981; Mushotzky et al. 1981; White & Sarazin 1988).

Variously interpreted as a system of galaxies in collision (Baade & Minkowski 1954; Rubin et al. 1977; Hu et al. 1983; Holtzman et al. 1992), two superposed galaxies with no interaction (De Young, Roberts, & Saslaw 1973), or a galaxy ejecting material (Burbidge & Burbidge 1965), NGC 1275 has proved to be a fertile testing ground for studies of the interactions between galaxies and their environments. The possibility that the cooling flow is the source of the emission-line gas, the young stellar population, and the active nucleus was explored by Sarazin & O'Connell (1983). At the accretion rates inferred, one expects conspicuous UV emission from young, massive stars, provided that the cooling gas is processed into stars and the initial mass function (IMF) is similar to the Galactic IMF. Because NGC 1275 may be deficient in massive stars, it was suggested that its IMF is skewed toward low-mass stars by unusual conditions in the inflow (Fabian, Nulsen, & Canizares 1982; Sarazin & O'Connell 1983). Ultraviolet imaging can yield valuable information about current and recent star formation and help constrain the IMF. Here we discuss the Ultraviolet Imaging Telescope (UIT) images of NGC 1275 obtained during the *Astro-1* mission.

2. DATA ACQUISITION

Details of the UIT are given by Stecher et al. (1992). It photographed the Perseus Cluster on 3 days during the mission. However, due to telescope jitter, only data obtained on the seventh day are of good quality. We have analyzed three $\sim$560 s exposures in each of the A1 ($\lambda_0 = 249$ nm, $\Delta\lambda = 115$ nm), B1 ($\lambda_0 = 152$ nm, $\Delta\lambda = 35$ nm), and B5 ($\lambda_0 = 160$ nm, $\Delta\lambda = 23$ nm) filters. Exposures through the B6 ($\lambda_0 = 150$ nm, $\Delta\lambda = 40$ nm) filter were very short (90 s). The full 40′ field of view encompassed the central portion of the Perseus Cluster.

Following initial data processing as described in Stecher et al. (1992), subimages 200 × 200 pixels; 4′ × 4′) centered on NGC 1275 were extracted from the full 2048 × 2048 frames. We removed sky backgrounds by fitting and subtracting a low-order polynomial to each line of every image. We inspected the resulting images and masked out bad pixels from film defects or cosmic-ray hits. The A1 filter data were of sufficient signal-to-noise ratio that we were able to perform ellipse fits to isophotes using the ELLIPSE task found in STSDAS (cf. Jedrzejewski 1987). An estimate of the contribution of the non-thermal point source to the galaxy luminosity was derived by the method of Smith et al. (1986). Intrinsic values stated below assume a Hubble constant, $H_0 = 100$ km s^{-1} Mpc^{-1}.

[1] Laboratory for Astronomy and Solar Physics, NASA/Goddard Space Flight Center, Code 681, Greenbelt, MD 20771.
[2] Visiting Observer at the Kitt Peak National Observatory of the NOAO operated by AURA, Inc., under contract with the NSF.
[3] Astronomy Department, University of Virginia, Charlottesville, VA 22903.
[4] Space Telescope Science Institute, 3700 San Martin Drive, Baltimore, MD 21218.
[5] National Research Council Postdoctoral Fellow.
[6] Hughes STX Corporation, NASA/Goddard Space Flight Center, Greenbelt, MD 20771.
[7] Department of Physics, University of Nevada, 4505 South Maryland Parkway, Las Vegas, NV 89154.
[8] National Radio Astronomy Observatory, Edgemont Road, Charlottesville, VA 22903.

3. MORPHOLOGY AND COLOR DISTRIBUTION

The underlying galaxy in NGC 1275 is presumed to be an elliptical with an associated system of ionized filaments (the LV system). High-velocity gas (the HV system), superposed near position angle $\sim 300°$, is usually interpreted as a late-type galaxy in the foreground (Rubin et al. 1977; Boroson 1990). Both systems are preferentially concentrated on the northern half of NGC 1275 (Cowie et al. 1983; Caulet et al. 1992). A bright mid-F star (Hughes & Robson 1991) is located 8".4 northeast of the nucleus. NGC 1275 exhibits a strong blue color gradient [$\Delta(B-V) \sim 1$ mag within an 80" radius], and is *bluer* toward the nucleus—contrary to the color gradient in most elliptical galaxies (Romanishin 1987; McNamara & O'Connell 1992).

Figure 1 (Plate L29) is the image taken in the A1 filter, with the V-band contours from Smith & Heckman (1989) superposed. The point-spread function (PSF) in this exposure has FWHM = 4".2, but has broad wings. The near-UV morphology is clearly not as azimuthally symmetric as that at longer wavelengths. It is extended in the position angles where the LV and HV filaments are brightest as found by Caulet et al. (1992). Compared with the optical/IR, the UV morphology is more strongly affected by hot stars ($T_e > 12{,}000$ K) and/or internal extinction. Emission lines are not expected to be important in our UV bands. C IV λ1550 is present in the B1 and B5 filters but is not found in off-nucleus *IUE* spectra (Nørgaard-Nielsen, Hansen, & Jørgensen 1990), nor is it expected to be strong at the characteristic temperatures of the HV and LV regions.

To study the asymmetry, we fitted ellipses to the near-UV (NUV) image and used these to construct a symmetric elliptical model which we subtracted from the image, yielding the residual UV light shown in Figure 2 (Plate L30). The residual light is spatially coincident with the extended Hα emission (Caulet et al. 1992, Fig. 3). It appears that the excess UV light is associated with some areas in the LV and HV systems, though the detailed correspondence is uncertain because of our broad PSF and the difficulties in registering the optical and UV observations. The total light from the asymmetric features at $r > 4''$ is $\sim 5\%$ of the total NUV luminosity. The bright knot immediately northeast of the nucleus could be the foreground F star (Hughes & Robson 1991) or UV light associated with HV system Hα emission. The enhanced region at $r = 20''$, P.A. = 62° is probably the bright young star cluster in the LV system (the "SF cluster"; Shields & Filippenko 1990).

The light distribution of the galaxy NGC 1275 in the far-UV (FUV) images (B1 and B5 filters) is even less azimuthally symmetric than the NUV light (see Fig. 3 [Pl. L31]). The central point source contributes a larger fraction of the FUV light. The bright knot at $r = 20''$, P.A. $\sim 62°$ is coincident with the SF cluster, as in the NUV. This object is much brighter in the FUV than in the NUV and is bluer than the body of the galaxy.

The westernmost concentration (40" northwest) of residual light is coincident with a region of HV system Hα emission. The excess flux in a 10" aperture there is $\sim 1.1 \times 10^{-16}$ ergs s^{-1} cm^{-2} Å^{-1}. This is only a factor of 2 smaller than expected from the Hα observations (Caulet et al. 1992), which yield an intrinsic L(Hα) $\sim 2.4 \times 10^{40}$ ergs s^{-1} in this area (their "regions 10 and 11") and the theoretical models described below to predict the UV continuum from a young population large enough to ionize the gas. (We adopted the extinction value in Table 3 for this estimate.) It is therefore probable that we have detected the stellar population which has been presumed to exist in the HV system (Rubin et al. 1977). The only other reported detections of starlight in the HV system are of 5000 Å continuum and Ca II λ8498 absorption (Meaburn et al. 1989; Boroson 1990). Based on our UV detection, the corresponding V-band magnitude is ~ 21, or roughly consistent with the continuum measurements of Meaburn et al. (1989).

Figure 4 gives the NUV surface brightness profile derived by fitting ellipses to the image (corrected for Galactic extinction

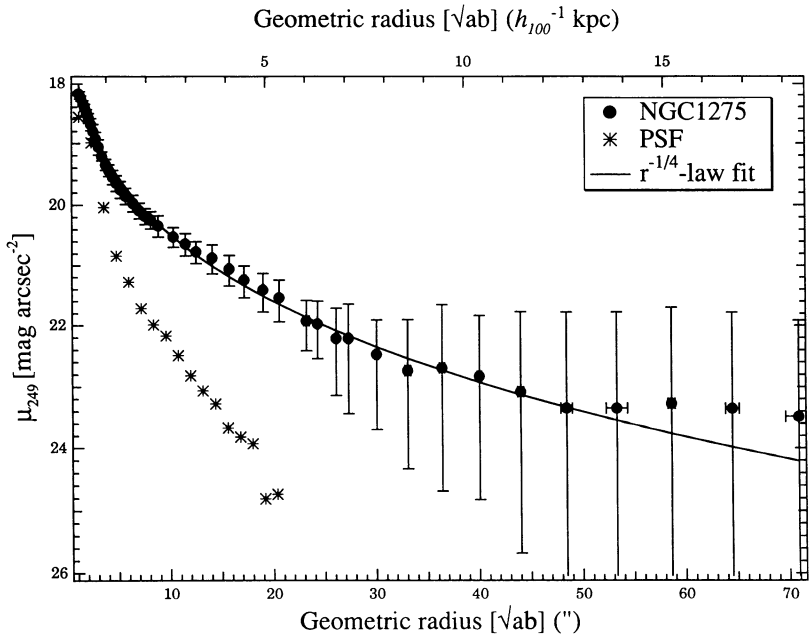

FIG. 4.—Surface brightness vs. geometric radius for NGC 1275 in the A1 filter (249 nm), from ellipses and an $r^{-1/4}$ law fit to the data. The point-spread function obtained from five stars in this image is plotted also, with a central surface brightness scaled to that of NGC 1275. Magnitudes were corrected for Galactic extinction. The error bars reflect the rms scatter of intensity along the fitted ellipse converted to magnitudes.

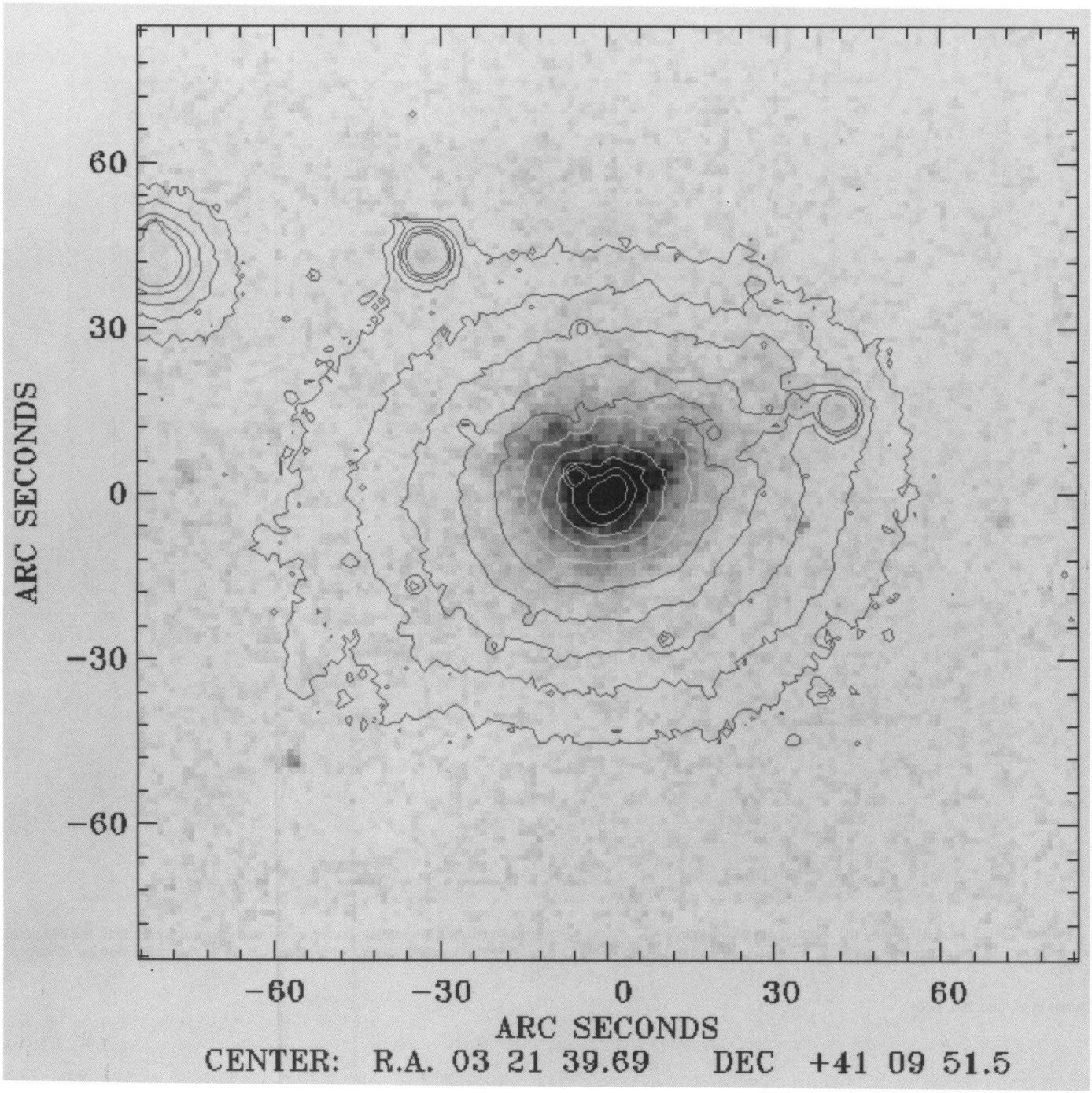

FIG. 1.—UIT NUV (249 nm) image of NGC 1275. North is at the top, and east is to the left. V-band contours (starting at 23 mag arcsec^{-2}, at 0.735 mag intervals) are overlaid. The range of displayed UV intensities is $0 < I < 3 \times 10^{-17}$ ergs s^{-1} cm^{-2} Å^{-1}. The galaxy centered $\sim 80''$ northeast of NGC 1275 (and truncated in the figure) was not detected by the UIT (Hintzen et al. 1992).

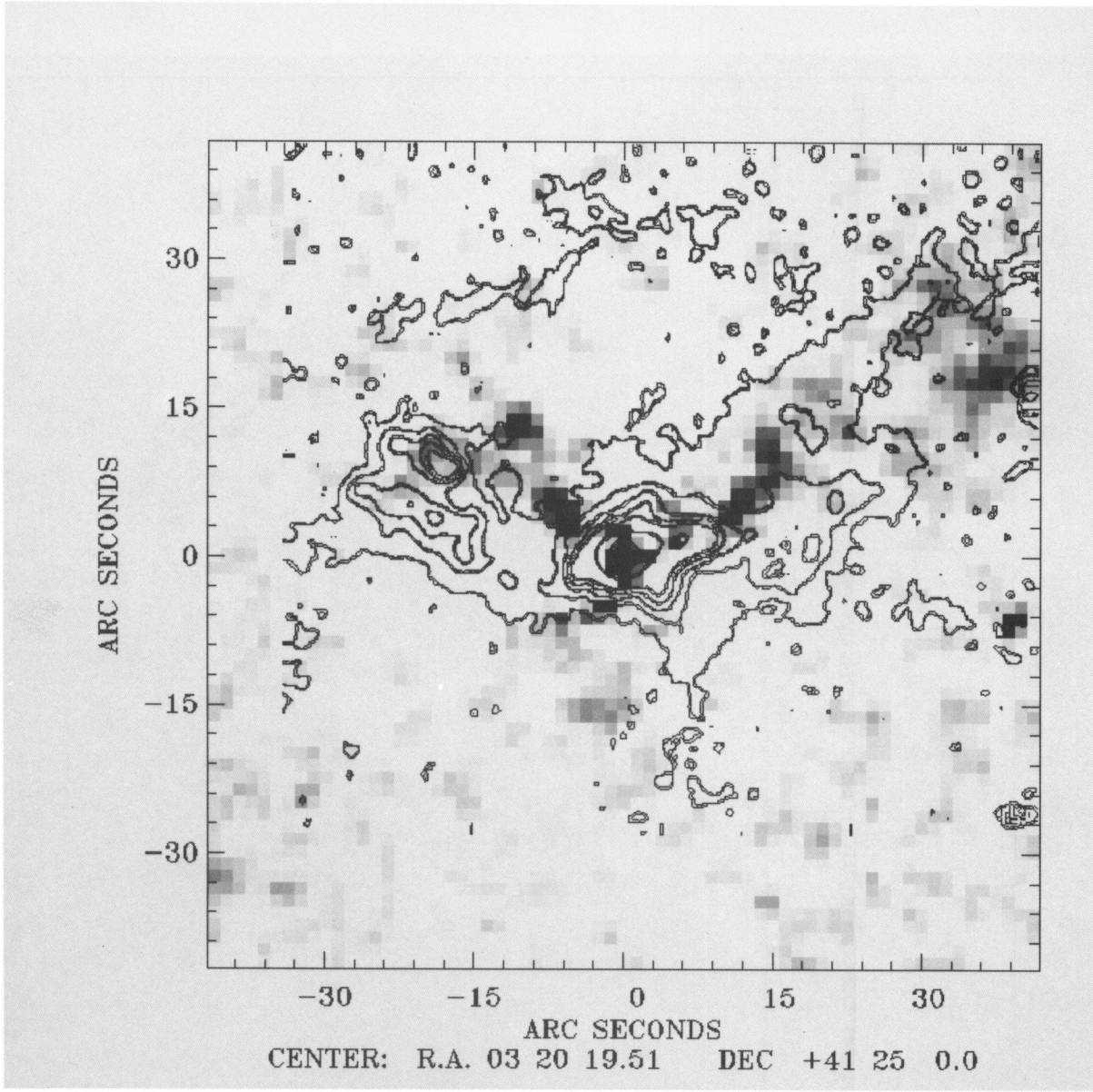

FIG. 2.—NUV image showing the residual morphology of NGC 1275 after a smooth elliptical light distribution constructed from ellipse fits to the 249 nm data was subtracted. Image orientation, scale, and range of displayed intensities are as in Fig. 1. Overlaid contours represent the LV Hα emission-line gas (Caulet et al. 1992).

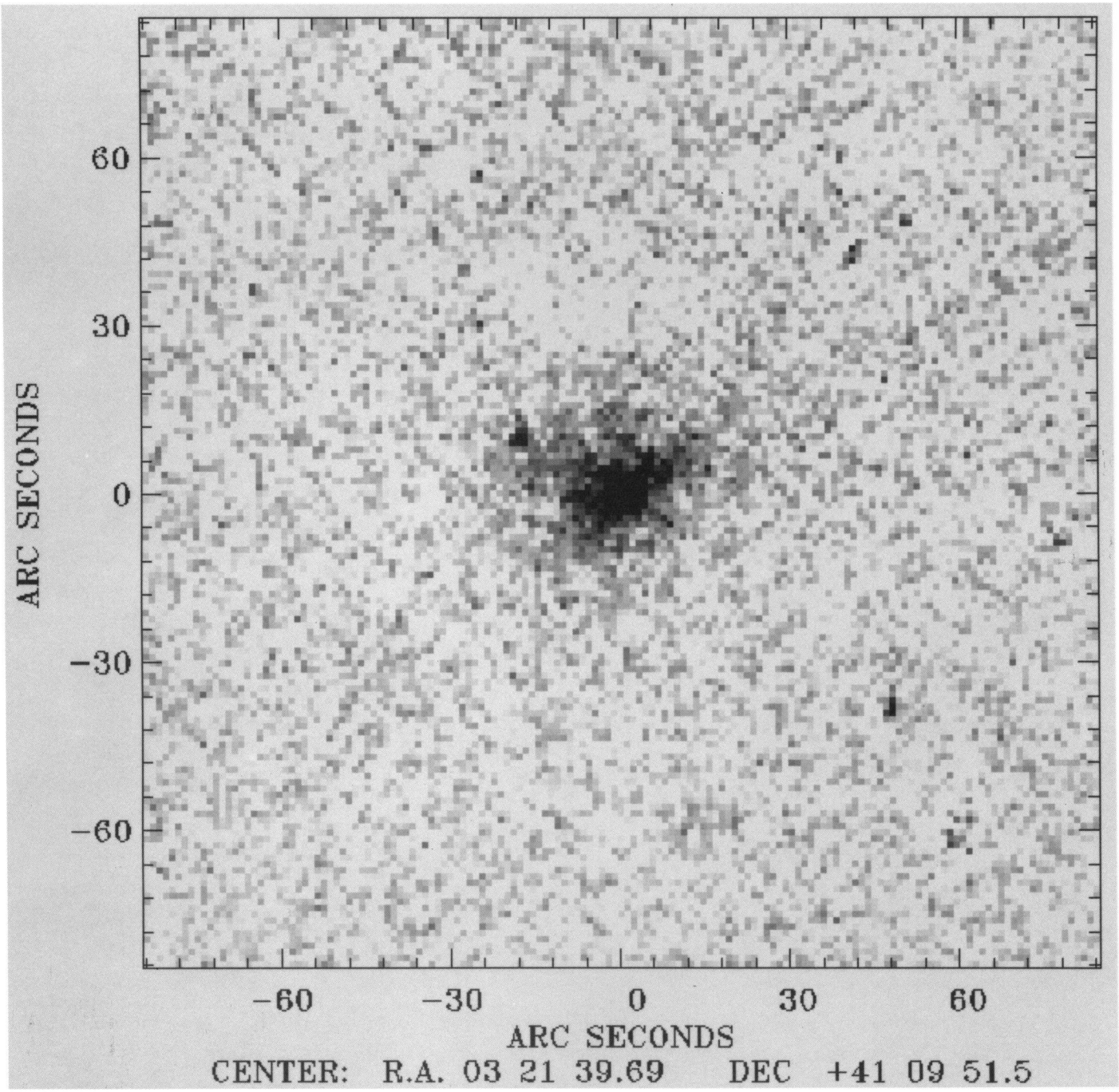

FIG. 3.—B1 (152 nm) image of NGC 1275. Image orientation and scale are as in Fig. 1, but displayed UV intensities are $0 < I < 2.5 \times 10^{-17}$ ergs s^{-1} cm^{-2} $Å^{-1}$.

SMITH et al. (see 395, L50)

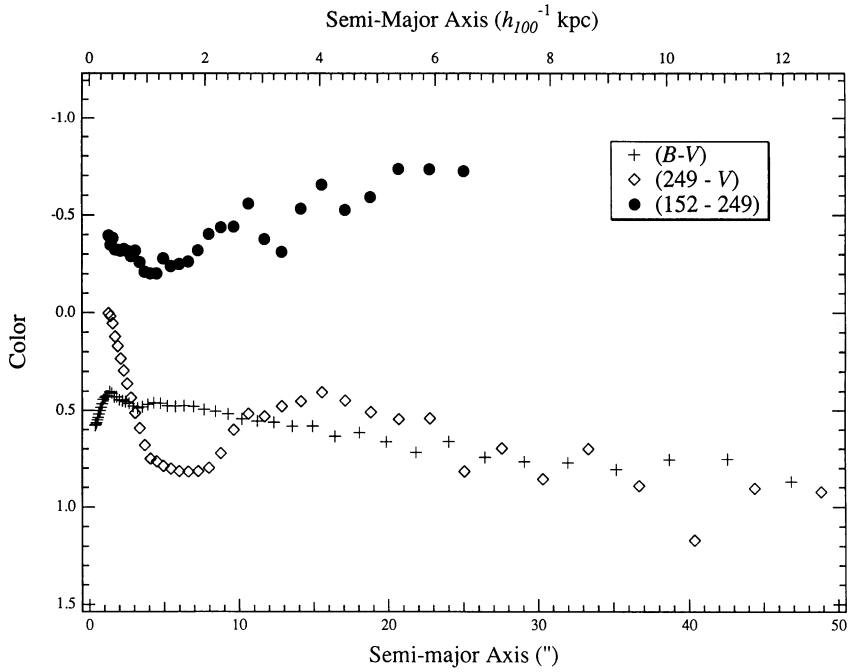

FIG. 5.—Plot of the variation of the $(249-V)$, $(B-V)$, and $(152-249)$ colors with semimajor axis. All colors were corrected for Galactic extinction only. The V-image was smoothed to the UIT resolution before deriving its profile. The UV profiles are truncated at radii where the measured ellipse intensities became comparable to their rms scatter.

only). UV fluxes were converted to surface brightnesses adopting

$$m_\lambda = -2.5 \log f_\lambda - 21.1 - A_\lambda ,$$

where f_λ is in ergs s^{-1} cm^{-2} $Å^{-1}$, and A_λ is the extinction, based on Table 3. We used these fits to model the NUV image as either an $r^{-1/4}$ law spheroid or an exponential disk with an added point source to assess the contribution of the nucleus to our photometry. Good fits (reduced $\chi_\nu^2 \approx 1$) were obtained with only 2%–8% of the light in the NUV arising in the point source. We cannot distinguish between the two models, however. Similar analysis of the B1 image indicates that ~20% of the FUV light arises in the nucleus. In the V band, the point source contributes only ~3% of the light (Smith & Heckman 1989).

Figure 5 presents color profiles from our UV surface photometry and corresponding measures of the B and V CCD images of Smith & Heckman (1989). The colors are defined as $(249-V) \equiv (m_{\lambda 249} - V)$, and $(152-249) \equiv (m_{\lambda 152} - m_{\lambda 249})$, etc. Plotted colors were corrected for foreground Galactic reddening (see below) but not for internal extinction, and the V profile was smoothed to the UIT resolution. There are significant gradients in $(249-V)$ and $(B-V)$ across the face of NGC 1275, with the inner regions bluer than the outer. The overall range in $(249-V)$ is ~0.8 mag, within 8 h_{100}^{-1} kpc. The sense of the gradient is the same as that reported from *UBVRI* photometry (Romanishin 1987; Smith & Heckman 1989; Holtzman et al. 1992; McNamara & O'Connell 1992). However, NGC 1275's colors are much bluer than, and the gradients are larger than and opposite to, those normally found in giant ellipticals (e.g., Peletier et al. 1991). The bluest region (excluding the nucleus) is at $r \sim 15''$; inside this radius the color becomes redder. There is a similar redward trend in $(152-249)$ in this region but not in $(B-V)$. The small amplitude in the $(152-249)$ index at $r \geq 8''$ suggests that this is a stellar population, not an extinction effect; but the photometry is not accurate enough to be certain. The spike in $(249-V)$ at $r < 4''$ indicates the AGN, but color profiles here are unreliable because of PSF effects.

4. STAR FORMATION IN NGC 1275

Our synthetic aperture photometry is summarized in Table 1. We give the integrated fluxes for centered apertures 40″ and 80″ in diameter. At the former (latter) diameters, the galaxy surface brightness has fallen to within 1 $\sigma_{\rm sky+fog}$ background on the B1 (A1) image. Table 2 gives the corresponding colors after correction for reddening and the AGN. Tables 1 and 2 also list 12″ aperture measurements for the SF cluster. We searched for the compact blue star clusters found on *HST* PC images by Holtzman et al. (1992). Our resolution is inadequate to distinguish them readily. Nevertheless, we attempted to measure their colors by photometry with a 7.″2 diameter aperture at the locations of 33 clusters which were at least 4 UIT PSF radii from the nucleus. The mean values for these measurements are given in the tables. Stecher et al. (1992) discuss the UIT calibration.

Since NGC 1275 is at low Galactic latitude and is known to contain significant internal dust, extinction corrections are crucial. Table 3 lists our assumptions for foreground and internal extinction. The best estimates for internal extinction come from Balmer line strengths in the LV regions (Kent & Sargent 1979; Shields & Filippenko 1990). They indicate internal $E(B-V) \sim 0.26$, if we adopt the Burstein & Heiles (1982) value in Table 3 for the Galactic extinction. It is not clear that this is representative of the body of the galaxy. The gaseous filaments and clusters recently formed from them could be anomalously rich in dust. Furthermore, *IUE* observations of star-forming galaxies often imply smaller effective $E(B-V)$ in the ultraviolet than would be inferred from optical-band extinction estimates

TABLE 1

OBSERVED FLUXES ($\times 10^{-15}$ ergs s^{-1} cm^{-2} Å^{-1})[a]

BANDPASS (1)	NGC 1275 GLOBAL 40″ (2)	NGC 1275 GLOBAL 80″ (3)	SF CLUSTER 12″ (4)	$\Delta\alpha = 9''$, $\Delta\delta = 2''$ *IUE* APERTURE (5)	⟨*HST* CLUSTERS⟩ 7.″2 (6)
f_λ(249 nm) A1	7.45	12.30	0.39	1.39	0.21
f_λ(152 nm) B1	9.74	14.72	0.81	1.99	0.30
f_λ(162 nm) B5	8.49	12.76	0.34	1.55	...
$f_\lambda(V)$	26.10	40.60	0.45	4.71	0.0084*

[a] The measurements include contributions from the AGN, but not nearby objects or plate defects. Cols. (2) and (3) are for circular apertures with the listed diameters. Col. (4) lists the flux from an aperture centered at P.A. = 62°, $r = 20''$, on the Shields & Filippenko cluster. Col. (5) gives the flux from simulation of the *IUE* aperture (roughly $10'' \times 20''$) rotated to a position angle of $-14°$ and centered 9″ west, 2″ north of the intensity peak. Col. (6) lists mean flux referenced to the local background, for 33 positions coincident with *HST* PC blue clusters (see § 4). *V* data are from Smith & Heckman 1989; the asterisk denotes mean data from Holtzman et al. 1992 measured through a 0.″18 diameter aperture.

(O'Connell 1990), either because the UV preferentially emerges from low-extinction regions or because the dust is mixed with the stars. In fact, Hu (1992) obtains internal $E(B-V) \sim 0.17$ from the Lyα/Hβ ratio. We adopt the Kent & Sargent (1979) value for reference but regard the internal UV extinction as very uncertain and consider mainly the direction, rather than the magnitude, of the reddening vectors in our intepretation.

Figure 6 shows our photometry of NGC 1275 on a UV color-color diagram. The measured colors of Large Magellanic Cloud (LMC) clusters from Cassatella, Barbero, & Geyer (1987) are included, and the colors for various normal types of stars are indicated. Two sets of synthetic models for stellar populations with ages of 0–1000 Myr are also shown. One of these was calculated by the methods of Lequeux (1979) and Lequeux et al. (1979) (but with a shallower upper mass exponent of -2) to derive theoretical colors of single-generation populations corresponding to the evolutionary tracks of Maeder (1990) and Maeder & Meynet (1988), and the model stellar atmospheres of Kurucz (1991). For ages $\gtrsim 50$ Myr, these models underestimate the *V*-band contribution of cool, evolved stars. The other model set is empirical, based on *IUE* spectra compiled by Fanelli et al. (1992) and composite color-magnitude diagrams for a normal IMF (O'Connell 1983). Both single-generation and constant star formation models are included. The scatter indicates the current uncertainties in such model building. The offset in $(152-249)$ between the models and the LMC clusters may reflect FUV blanketing differences between the models (solar abundance) and the LMC clusters ($Z \sim 0.5\ Z_\odot$).

The observed large-aperture UV colors of NGC 1275 are consistent with those of an early A star or an LMC cluster with an age of ~ 250 Myr. A dereddening vector corresponding to removal of our adopted total extinction if all the dust lies in the foreground is shown in Figure 6 (the spot marked "G" indicates Galactic reddening only). The maximum correction for uniformly mixed dust and stars would be a similar vector about 0.25 mag shorter. For the plausible range of internal extinction, $E(B-V) \sim 0$–0.3, the intrinsic large-aperture NGC 1275 colors are consistent with a single generation of an age ~ 70–150 Myr or a population which formed continuously from ~ 1000 Myr until 50–70 Myr ago. Larger extinction corrections would imply intrinsic colors that do not agree well with any models. Overall, the colors and adopted reddening law are not consistent with models in which star formation with a normal IMF has occurred during the last ~ 50 Myr. The UV photometry therefore supports the other evidence cited in § 1 on the absence of OB main-sequence stars despite a dominant population of less massive objects ($M \lesssim 5\ M_\odot$). It is unlikely that all the light in our aperture arises from the most recent episode of star formation. Wirth et al. (1983) estimated that $\sim 30\%$ of the light at 5050 Å can be attributed to an old (type K or later) stellar population. We have added a vector to the 80″ aperture point in Figure 6 to show the effects of varying the fraction of the *V* light assumed to preexist before the onset of the most recent star formation. The NUV and FUV magnitudes are not significantly altered ($\Delta m \leq 0.1$) by the old population. We estimate the total mass of this intermediate-age population from the FUV luminosity, which is the least con-

TABLE 2

NGC 1275 UV COLORS[a]

APERTURE	OBSERVED COLORS (152−249)	OBSERVED COLORS (152−*V*)	+GALACTIC EXTINCTION (152−249)	+GALACTIC EXTINCTION (152−*V*)	+INTERNAL + GALACTIC (152−249)	+INTERNAL + GALACTIC (152−*V*)
NGC 1275 (40″)	−0.14	+1.28	−0.28	0.40	−0.46	−0.90
NGC 1275 (80″)	−0.04	+1.31	−0.18	0.43	−0.36	−0.87
S&F cluster	−0.79	−0.64	−0.93	−1.52	−1.11	−2.82
IUE aperture	−0.39	+0.94	−0.53	0.06	−0.71	−1.24
⟨*HST* clusters⟩	−0.39	...	−0.53	...	−0.71	...

[a] The listed colors were corrected for the point-source contribution using the percentages derived from image modeling (§ 2). The SF cluster, *IUE* aperture, and mean *HST* PC cluster colors are not corrected for point-source contributions, since they are small-aperture measurements, centered off-nucleus.

TABLE 3

EXTINCTION CORRECTIONS[a]

Bandpass	Galactic (mag)	Galactic + Internal (mag)
A1 (249 nm)	1.28	3.18
B1 (152 nm)	1.42	3.50
B5 (162 nm)	1.41	3.48
V	0.54	1.32

[a] $E(B-V) = 0.17$ (Burstein & Heiles 1982) for Galactic extinction, $E(B-V) = 0.26$ (Shields & Filippenko 1990) for the intrinsic extinction, and the extinction law of Savage & Mathis 1979 are assumed.

taminated by older light. A reddening of $E(B-V) = 0.2$ provides a good fit to our spectral synthesis model for continuous star formation ending ~ 70 Myr ago. This implies an absolute UV magnitude of $M_\lambda(1500) = -21.6$ in our 80″ aperture and a V-luminosity for the intermediate-age population of $\sim 4.7 \times 10^{10}\ L_\odot$. The mass is $\sim 3 \times 10^{10}\ M_\odot$, and the corresponding star formation rate is $\sim 20\ M_\odot\ \mathrm{yr}^{-1}$. An alternative interpretation as a single-generation population of either 70 or 200 Myr age leads to a mass of $\sim 1.0 \times 10^{10}\ M_\odot$. If these populations formed in a period $\sim 10\%$ of their present ages, the implied star formation rates are 500–1500 $M_\odot\ \mathrm{yr}^{-1}$, comparable to the most luminous *IRAS* starburst systems.

The UV colors are also consistent with star formation continuing to the present if the IMF truncates for large masses (Sarazin & O'Connell 1983). A model with $m_{\mathrm{upper}} = 5\ M_\odot$ and an age of 4 Gyr is consistent with the UV colors if $E(B-V) = 0.2$. The implied mass is $\sim 6 \times 10^{10}\ M_\odot$, and the star formation rate is 15 $M_\odot\ \mathrm{yr}^{-1}$.

Nørgaard-Nielsen et al. (1990) obtained bluer UV colors from *IUE* spectra for a region at 10″ from the nucleus. Such colors indicate normal IMF star formation continuing to the present. However, the Nørgaard-Nielsen et al. data had low signal-to-noise ratios, and they had to estimate the V-band flux from very narrow band photometry in the literature. Consequently, their photometry is uncertain. The UIT colors for the same region are shown in Figure 6. They are only slightly bluer than the large-aperture colors.

The SF cluster is significantly bluer (Fig. 6) than the main body of NGC 1275 but is likewise not consistent with a very young, normal IMF population. In this case, however, strong Balmer lines (Shields & Filippenko 1990; Holtzman et al. 1992) indicate the presence of ionizing OB stars, which do not persist more than ~ 5 Myr. A total extinction correction corresponding to $E(B-V) \sim 0.6$ would move the cluster's UV colors into agreement with such young populations. However, the nominal extinction, $E(B-V) \sim 0.43$, already appears to overcorrect the observed $(B-V)$ (Shields & Filippenko 1990), so a larger value is not appropriate. It is more likely that the region we observed contains several generations, with ages spread from less than 5 up to several hundred Myr. Colors for such populations are consistent with the observed SF UV colors and the nominal extinction. There may actually be several clusters within our 12″ aperture. Shields, Filippenko, & Basri (1990) found that there were multiple Hα velocity components in the direction of the SF cluster, supporting this interpretation. The mean UV colors we obtain for the locations of the Holtzman et al. (1992) clusters are roughly 0.2 mag bluer than the galaxy as a whole but are less reliable than our other photometry, owing to coarse resolution. These values are, however, consistent with the age of several hundred Myr derived by Holtzman et al.

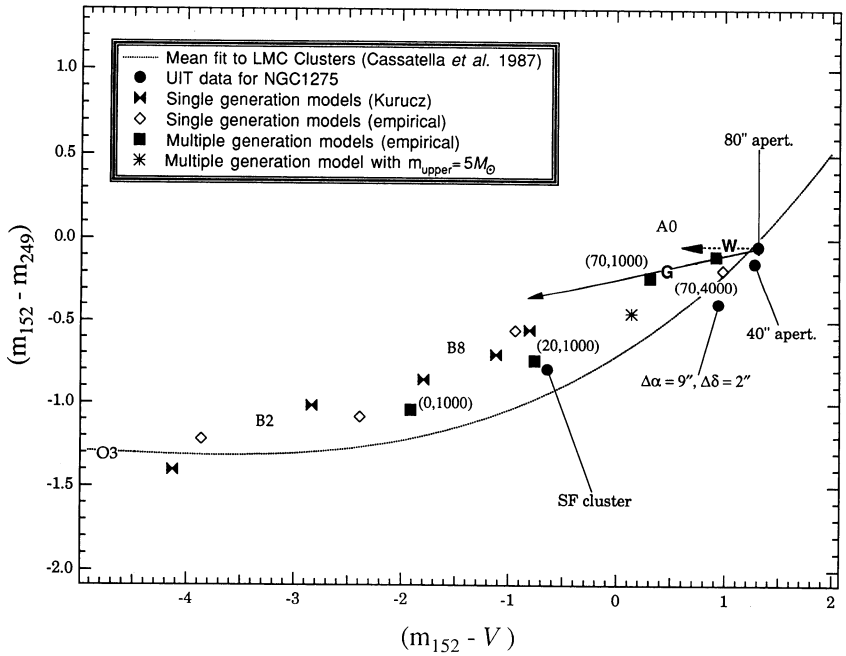

FIG. 6.—UV color-color diagram comparing UIT observations of NGC 1275 with stellar population models. The colors of several main-sequence stellar types are shown for reference. A reddening vector was added to the point for the 80″ aperture. The location "G" on the vector indicates the magnitude of Galactic extinction, while the total length represents our adopted internal + Galactic reddening. A vector indicating the effect of varying the amount of light from a preexisting population of old stars was added to the 80″ point. The location "W" on this vector shows the effect of removing a 30% contribution of V light by the old population (see § 4) on the color of the most recent star-forming epoch, while the total length represents the removal of a 50% contribution. The single-generation model ages are (*left to right*) 0, 20, 60, 120, and 200 Myr for the Kurucz models, and 0, 20, 70, and 200 Myr for the empirical models. The (ending, onset) ages in Myr are given for the multiple-generation models; for the truncated IMF model, they are (0, 4000).

5. DISCUSSION

The UIT images confirm that extensive star formation has occurred throughout NGC 1275 in the last Gyr. About 5% of the NUV continuum is associated with the LV and HV emission-line systems superposed on the smooth UV light distribution of the elliptical galaxy. Subject to uncertainties in extinction and the reddening law, the UV colors are consistent with a single burst of star formation $\sim$70–250 Myr ago or with continuous star formation with a normal IMF ending $\sim$50–70 Myr ago. Star formation with a normal IMF has not been widespread since that time (past 50–70 Myr), although it has occurred in localized regions (e.g., the SF cluster). Burst models imply star formation rates of 500–1000 $M_\odot$ yr^{-1}, whereas rates for the continuous models are only $\sim$20 $M_\odot$ yr^{-1}. The colors are also consistent with ongoing star formation if the IMF is truncated at $M \gtrsim 5\ M_\odot$.

These results can fit either the merger or the cooling-flow interpretation of NGC 1275. In the merger picture, an interaction $\sim$100 Myr ago with a presumably gas-rich companion induced widespread star formation as well as formation of a central swarm of luminous star clusters (Holtzman et al. 1992). Little star formation has occurred since. The LV filaments would be the products of cold clouds stripped from infalling gas-rich systems and heated by the hot intracluster medium in the merger scenario (Sparks, Macchetto, & Golombek 1989). The presence of the cooling flow would be only incidental, and the endpoint of the cooling matter, $\lesssim 50\ M_\odot$ yr^{-1} in the 80″ UIT aperture (White & Sarazin 1988), remains to be accounted for. It is possible that it resides in small, cool interstellar clouds (White et al. 1991). In the cooling-flow picture, infalling gas produces the LV filament system, and star formation continues with a truncated IMF at a rate sufficient to consume most of the cooling matter. Given the uncertainties, the X-ray and UV mass-flow estimates are in reasonable agreement. In this picture, the uniform colors of the brighter Holtzman et al. (1992) clusters would result from truncated main sequences rather than a uniform age. Neither interpretation explains the HV emission-line system.

We thank M. Fanelli for his UV spectral synthesis models and software, and the anonymous referee for his/her helpful suggestions. This research was supported in part by grants NAG5-700 and NAGW-2596 to the University of Virginia.

REFERENCES

Baade, W., & Minkowski, R. 1954, ApJ, 119, 215
Boroson, T. 1990, ApJ, 360, 465
Burbidge, E. M., & Burbidge, G. R. 1965, ApJ, 142, 1351
Burstein, D., & Heiles, C. 1982, AJ, 87, 1165
Cassatella, A., Barbero, J., & Geyer, E. H. 1987, ApJS, 64, 83
Caulet, A., Woodgate, B. E., Brown, L. W., Gull, T. R., Hintzen, P., Lowenthal, J. D., Oliversen, R. J., & Ziegler, M. M. 1992, ApJ, 388, 301
Cowie, L. L., Hu, E. M., Jenkins, E. B., & York, D. G. 1983, ApJ, 272, 29
De Young, D. S., Roberts, M. S., & Saslaw, W. C. 1973, ApJ, 185, 809
Fabian, A. C., Hu, E. M., Cowie, L. L., & Grindlay, J. 1981, ApJ, 248, 47
Fabian, A. C., Nulsen, P. J., & Canizares, C. R. 1982, MNRAS, 201, 933
———. 1984, Nature, 310, 733
Fanelli, M. N., O'Connell, R. W., Burstein, D., & Wu, C.-C. 1992, ApJS, in press
Gear, W. K., Gee, G., Robson, E. I., & Nolt, I. G. 1985, MNRAS, 217, 281
Heckman, T. M. 1981, ApJ, 250, L59
Heckman, T. M., Baum, S. A., van Breugel, W. J. M., & McCarthy, P. 1989, ApJ, 338, 48
Heckman, T. M., Miley, G. K., & Green, R. F. 1984, ApJ, 281, 525
Hintzen, P., et al. 1992, in preparation
Holtzman, J. A., et al. 1992, AJ, 103, 691
Hu, E. M. 1992, ApJ, 391, 608
Hu, E. M., Cowie, L. L., Kaaret, P., Jenkins, E. B., York, D. G., & Roesler, F. L. 1983, ApJ, 275, L27
Hughes, D. H., & Robson, E. I. 1991, MNRAS, 249, 560
Jedrzejewski, R. 1987, MNRAS, 226, 747
Kent, S. M., & Sargent, W. L. W. 1979, ApJ, 230, 667
Kurucz, R. 1991, in Precision Photometry: Astrophysics of the Galaxy, ed. A. G. D. Philip, A. R. Upgren, & K. A. Janes (Schenectady: Davis), preprint
Lequeux, J. 1979, A&A, 80, 35
Lequeux, J., Peimbert, M., Rayo, J. F., Serrano, A., & Torres-Peimbert, S. 1979, A&A, 80, 155
Lynds, C. R. 1970, ApJ, 159, L151
Maeder, A. 1990, A&AS, 84, 139
Maeder, A., & Meynet, G. 1988, A&AS, 76, 411
McNamara, B. R., & O'Connell, R. W. 1992, ApJ, 393, 579
Meaburn, J. Allan, P. M., Clayton, C. A., Marston, A. P., Whitehead, M. J., & Pedlar, A. 1989, A&A, 208, 17
Minkowski, R. 1957, in IAU Symp. 4, Radio Astronomy, ed. H. C. van de Hulst (Cambridge: Cambridge Univ. Press), 107
Mushotzky, R. F., Holt, S. S., Smith, B. W., Boldt, E. A., & Serlemitsos, P. J. 1981, ApJ, 244, L47
Nørgaard-Nielsen, H. U., Hansen, L., & Jørgensen, H. E. 1990, A&A, 240, 70
O'Connell, R. W. 1990, in Windows on Galaxies, ed. G. Fabbiano, J. S. Gallagher, & A. Renzini (Dordrecht: Kluwer), 39
———. 1983, ApJ, 267, 80
Peletier, R. F., Davies, R. L., Illingworth, G. D., Davis, L., & Cawson, M. 1991, AJ, 100, 1091
Romanishin, W. 1987, ApJ, 323, L113
Rubin, V. C., Ford, W. K., Peterson, C. J., & Oort, J. H. 1977, ApJ, 211, 693
Sarazin, C. L., & O'Connell, R. W. 1983, ApJ, 268, 552
Savage, B. D., & Mathis, J. S. 1979, ARA&A, 17, 73
Seyfert, C. K. 1943, ApJ, 97, 28
Shields, J. C., & Filippenko, A. V. 1990, ApJ, 353, L7
Shields, J. C., Filippenko, A. V., & Basri, G. 1990, AJ, 100, 1805
Smith, E. P., & Heckman, T. M. 1989, ApJ, 341, 658
Smith, E. P., Heckman, T. M., Bothun, G. D., Romanishin, W., & Balick, B. 1986, ApJ, 306, 64
Sparks, W. B., Macchetto, F., & Golombek, D. 1989, ApJ, 345, 153
Stecher, T. P., et al. 1992, ApJ, 395, L1
White, D. A., Fabian, A. C., Johnstone, R. M., Mushotzky, R. F., & Arnaud, K. A. 1991, MNRAS, 252, 72
White, R. E., & Sarazin, C. L. 1988, ApJ, 335, 688
Wirth, A., Kenyon, S. J., & Hunter, D. A. 1983, ApJ, 269, 102